 doi:10.20944/preprints201909.0313.v1

Communication

Structural Flexibility of Peripheral Loops and Extended C-Term Domain of Short Length Substrate Binding Protein from *Rhodothermus marinus*

Ji-Eun Bae[1,2], In Jung Kim[3], Yongbin Xu[4,5] and Ki Hyun Nam[3,6,*]

[1] School of Life Sciences, KNU Creative BioResearch Group, Kyungpook National University, Daegu 41566, Republic of Korea
[2] KNU Institute for Microorganisms, Kyungpook National University, Daegu 41566, Republic of Korea
[3] Division of Biotechnology, Korea University, Seoul, 02841, Republic of Korea
[4] Department of Bioengineering, College of Life Science , Dalian Minzu University , Dalian 116600 , Liaoning , China
[5] Key Laboratory of Biotechnology and Bioresources Utilization , Dalian Minzu University , Ministry of Education, Dalian 116600 , China; yongbinxu@dlnu.edu.cn.
[6] Institute of Life Science and Natural Resources, Korea University, Seoul, 02841, Republic of Korea; structures@korea.ac.kr
* Correspondence: structures@korea.ac.kr; Tel.: 82-10-5208-5730 (K.H.N.)

Abstract: Substrate binding proteins (SBP) bind to specific ligands in the periplasmic region and bind to membrane proteins to participate in transport or signal transduction. Typical SBPs consist of two α/β domains and recognize the substrate by hinge motion between two domains. Conversely, short length *Rhodothermus marinus* SBP (named as RmSBP) exists around the methyl-accepting chemotaxis protein. We previously determined the crystal structure of RmSBP consisting of a single α/β domain, but the substrate recognition mechanism is still unclear. To better understand the short length RmSBP, we performed comparative structure analysis, computational substrate docking, and X-ray crystallographic study. RmSBP shares a high level of similarity in α/β domain with other SBP proteins, but it has a distinct topology in the C-term region. The substrate binding model suggested that conformational change in the peripheral region of RmSBP was required to recognize the substrate. We determined the crystal structures of RmSBP at pH 5.5, 6.0, and 7.5. RmSBP showed structural flexibility of the β1-α2 loop, β5-β6 loop, and extended C-term domain based on the electron density map and temperature B-factor analysis. These results provide information that will further the understanding of the function of the short length SBP.

Keywords: Substrate-binding protein; SBP; ABC transport; α/β-domain; *Rhodothermus arinus*

1. Introduction

The substrate binding protein (SBP) initially recognizes the substrate in periplasm and delivers this to membrane-bound subunits that catalyze concentrative uptake into cells [1-3]. SBP is part of the ATP-binding cassette transporter for substrate uptake, ion-gradient driving transporter, DNA binding protein as well as prokaryotic and eukaryotic channels and receptors [2-5]. In 1999, SBPs were classified based on the sequence similarity and topological arrangements of the β-sheet [6]. Recently, their classification has been updated into seven cluster groups based on a number of SBP structures deposited in Protein Data Bank, with each cluster having different structural characteristics [7]. These classified SBPs are involved in the unique molecular mechanism of the functioning of the transporters, channels, and signal transducers [7]. In the protein database, SBPs vary in size from approximately 25-70 kDa [4, 8]. These SBPs have little sequence similarity, but

 doi:10.20944/preprints201909.0313.v1

highly conserved overall three-dimensional structural folding [4]. The typical core of SBPs consists of two structural α/β domains, which are connected by a hinge region [8]. This shows that the unique architecture depends on the classified SBP cluster [7]. Substrate binding occurs between the two domains of SBP, stabilizing the closed form of the tightly packed protein with the substrate buried at the interface [4]. Typical SBP represents four structural states in the process of substrate recognition: (i) open-unliganded (ii) open-liganded (iii) closed-unliganded and (iv) closed-liganded[4].

Rhodothermusmarinus is thermohalophilic bacterium that grows optimally at 65°C [9]. We previously found the short length *R. marinus* SBP (named as RmSBP) consisting of 138 amino acids excluding the signal peptide [10]. This SBP gene is associated with methyl-accepting chemotaxis protein (MCP) gene, composed of single peptide, transmembrane, HAMP, and methyl-accepting transducer regions [10]. The same feature of SBP-MCP gene cluster from *R. marinus* are is also found in the *Rhodothermusprofundi*, *Rhodothermaceae bacterium* RA, *Salinibacterruber* strain DSM 13855, and *Salinibacterruber* strain M8 [10], indicating that short length of SBP often exists in the nature along with MCP. We previously determined the crystal structure of RmSBP at pH 4.5, which showed the presence of a single α/β domain [10]. RmSBP had a high similarity with C-terminal domain of *Sreptococcus pneumonia* SBP (PDB code: 3LFT, r.m.s. deviation of 2.3 Å for 149 Cα-atoms, named as SpSBP) and *Vibrio cholerae* serotype O1 SBP (3LKV, 2.5 Å for 149 Cα-atoms, named as VcSBP). The SpSBP and VcSBP structures interact with L-tryptophan and phenylalanine, respectively. The residues that recognize these amino acids are not conserved in RmSBP [10]. Although the structural features of RmSBP have been analyzed, the mechanism by which they recognize substrates is still unknown.

To better understand the substrate recognition of short length RmSBP, we performed comparative structure analysis, computational substrate docking, and X-ray crystallographic study. We described the topology between RmSBP and other SBP proteins and modeled potential substrate binding sites. The crystal structures of RmSBP at pH 5.5, 6.0, and 7.5 were determined at 1.5, 1.8, and 1.9 Å resolution, respectively. The structural flexibility of peripheral β1-α2 loop of RmSBP, as well as extended C-term regions was observed. Our results provide the beginning framework to understand the molecular function of short length SBP.

2. Materials and Methods

2.1. Comparative and computational analysis

The crystal structure of RmSBP at pH 4.5 (PDB code 5Z6V) was used as the starting point for the homolog search and substrate prediction study. The homolog model were searched and evaluated using Phyre2 sever[11]. The putative substrate binding site were predicted using the 3DLigandSite sever [12].

2.2. Protein Production

Cloning and protein production have been reported in previous studies [10]. Briefly, the RmSBP gene, excluding the signal peptide was cloned into pET28 and expressed in *E. coli* BL21 (DE3). Purified recombinant RmSBP was obtained by two-step purifications using Ni-NTA affinity and size exclusion chromatography. The final purified protein was stored in 10 mM Tris-HCl, pH 8.0 and 200 mM NaCl.

2.3. Crystallization

Purified RmSBP were concentrated to 20 mg/ml using centricon (Millipore, cutoff 10 kDa). Crystallization screen was performed using the sitting-drop vapor diffusion method at 20 °C using commercial crystallization kits. Briefly, 0.3 µl protein solution was mixed with 0.3 µl precipitant solution and equilibrated against 70 µl precipitant solution. Microcrystals were obtained following 3

 doi:10.20944/preprints201909.0313.v1

conditions: (i) 0.1 M Bis-Tris, pH 5.5, 0.2 M $MgCl_2$, and 25% (w/v) Polyethylene glycol 3,350, (ii) 0.1 M MES, pH 6.0 and 1.26 M Ammonium sulfate (iii) 0.1 M HEPES, pH 7.5 and 25% (w/v) Polyethylene glycol 3,350. Suitable crystals for X-ray diffraction were obtained using the sitting-drop vapor diffusion at 20 °C by mixing 1.5 µl protein solution and 1.5 µl precipitant solution, which was equilibrated against 200 µl reservoir solution with crystallization solutions mentioned above.

2.4. Diffraction data collection

X-ray diffraction data for RmSBP crystals were collected at 100 K on beamline 7A at the Pohang Light Source II (PLS-II, Korea)[13]. All crystals were equilibrated in a cryoprotectant solution containing reservoir supplemented with 20% (v/v) ethylene glycol and then flash-cooled with liquid nitrogen stream. The diffraction images were indexed, integrated, and scaled with the HKL2000 package [14]. The data collection statistics are listed in Table 1.

2.5. Structure Determination

The initial phases of RmSBPs were solved using the molecular replacement method using Phaser-MR in Phenix [15] with selenium-derived RmSBP at pH 4.5 (PDB code: 5Z6V) [10] as search model. Manual model building was performed with COOT program [16]. The model refinement was performed with Refmac5 [17] and Phenix refinement in Phenix [18]. The geometry of refined model was evaluated using MolProbity server [19]. The structure refinement statistics are listed in Table 1. Figures were generated with the PyMOL [20]. Structure factors and coordinates have been deposited in the Protein Data Bank (PDB) under PDB code 6K1W (pH 5.5), 6K1X (pH 6.0) and 6K1Y (pH 7.5).

3. Results

3.1. Computational analysis of RmSBP

Typical SBPs reported to date, recognize substrates between two domains [7], whereas RmSBP has one domain [10]. We previously suggested that these RmSBPs can recognize substrates alone or recognize the substrate with other partner proteins [10]. In both cases, we hypothesized that structural change of the peripheral region of the RmSBP was required to recognize the substrate molecule. To better understand the substrate recognition of RmSBP, we performed the comparative analysis and substrate docking studies using previously reported crystal structure of SBP (PDB code 5Z6V) as starting point model structure. The analysis using Phyre2 server provided 19 models similar to RmSBP and the expected 19 substrate binding sites. Among them, 9 models (PDB code: 2QH8, 3LFT, 5ER3, 6DSP, 5BRA, 3KSM, 2DRI, 5DTE, 4KZK, 4RS3, 8ABP) with TM-score of > 0.48 were used for this study, which were peptide or sugar binding SBPs (**Figure 1a**). These models consisted of α/β fold structures and had low sequence identity of 13-30% with RmSBP. The superimposition of RmSBP with other SBPs showed similarity for core α/β domain for 73-119 Cα atoms (with r.m.s. deviation of 1.753-2.133 Å) , whereas the topology of C-term residue showed difference in conformation (**Figure 1a**). In RmSBP, β6-strand in extended C-term domain formed an antiparallel β-sheet with the β5-stand of the α/β domain core. In addition, the α5- and α6-helixes of RmSBP flanked their α/β domain. In contrast, the C-term regions of other SBPs lied upward in the direction of the substrate binding site (**Figure 1a and Figure 1b**), which further connected with the partner α/β domain to recognize the target substrate. Therefore, the extended C-term domain of RmSBP had significantly distinct topology against other typical SBPs. Next, the prediction of the substrate binding site was performed using 3DlignadStie. Results showed that N-terminus (Glu27, Val28 and Thr28), α1-helix (Gln32 and Gln33), β3-α4 loop (Leu106 and Glu107) and β5-β6 loop (Lys150) in RmSBP were predicted to be substrate binding sites (**Figures 1c**). Among them, the conformational change of side chain of Gln32 and Gln33 could be possible, but large conformation change was difficult since the main chain was present in the stable helix formation. The Leu106 and Glu107, on the other hand, were located in sharp turn of β3-α4 loop, thus limiting large

Preprints (www.preprints.org) | NOT PEER-REVIEWED | Posted: 27 September 2019 doi:10.20944/preprints201909.0313.v1

conformational change. Based on the computational docking study, we considered that nonstructural N-terminus and β5-β6 loop of RmSBP could show structural flexibility.

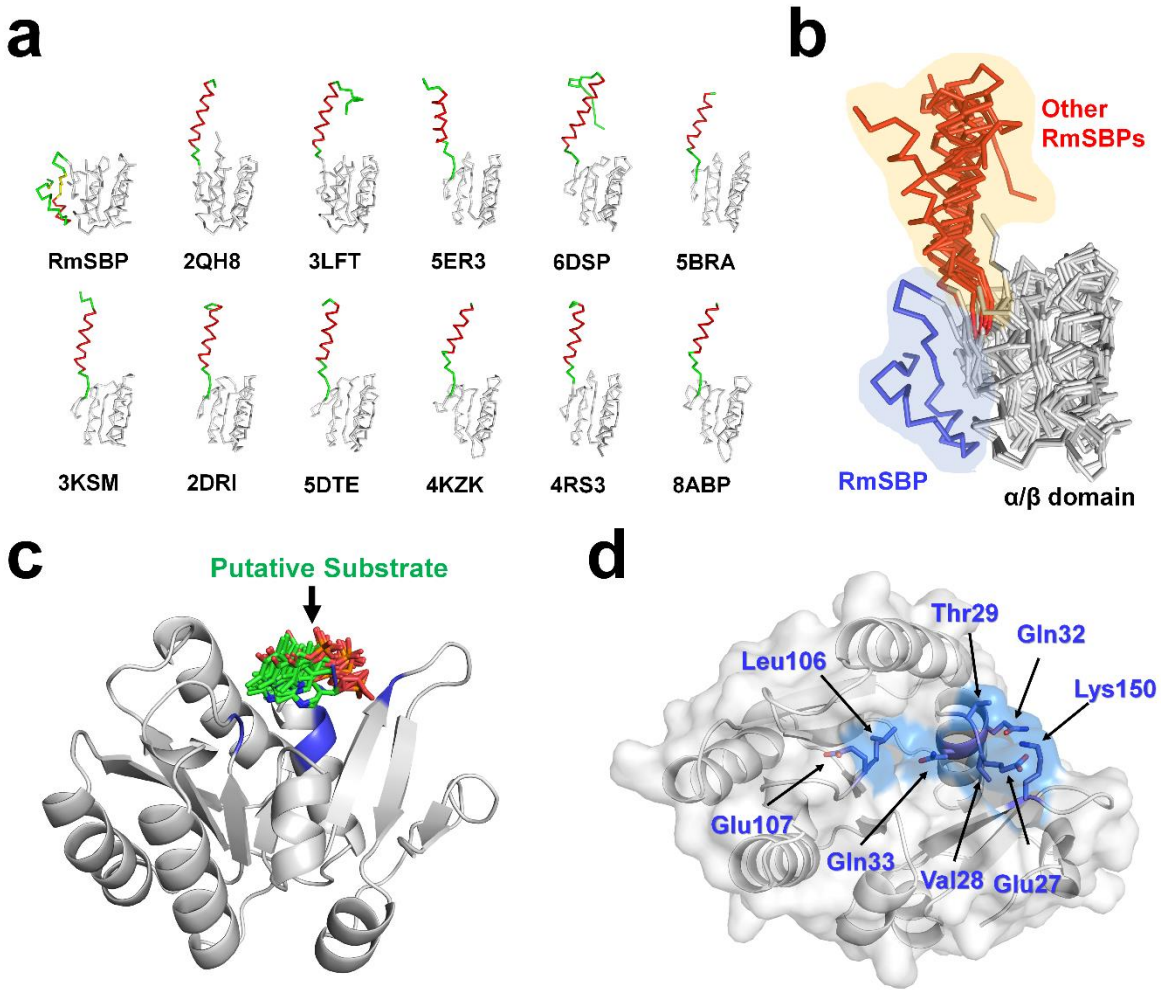

Figure 1. Computational analysis of RmSBP. (a) Comparative analysis of topology of RmSBP and other SBPs. α/β domain and C-term domain are indicated by grey and colored (yellow, green and red) ribbon. (b) Superimposition of RmSBP with structural homolog SBPs. (c) Computational prediction of the substrate binding on RmSBP. Total 15 PLP molecules have been laid on the α/β domain. (d) Predicted substrate recognition residues.

3.2. Crystal structures of RmSBPs

Our computational substrate docking study suggested that RmSBP might have the structural flexibility of peripheral loop region of α/β domain and C-term domain. However, in the previously reported structure of RmSBP at pH 4.5, the peripheral loops and α/β-fold of RmSBP exhibited a highly rigid structure (see below). As a result, there was no experimental evidence to prove the structural flexibility of RmSBP by computational analysis. To prove the computational analysis, we performed the extended crystallographic study to observe the structural flexibility of peripheral loops of the substrate recognition surface of RmSBP. We obtained RmSBP crystals at pH 5.5, 6.0 and 7.5, with different crystallization condition. Crystals of RmSBP at pH 5.5 and 7.5 belonged to the orthogonal space group $P2_12_12_1$, with similar unit-cell dimension of approximately a=46 Å, b=48 Å and c= 58 Å, occupying one molecule in the asymmetric unit (**Table 1**). Crystal of RmSBP at pH 6.0 belonged to the orthogonal space group $P2_122_1$, with unit cell dimension of 34 Å, 35 Å, and 115 Å,

 doi:10.20944/preprints201909.0313.v1

occupying one molecule in the asymmetric unit (**Table 1**), whereas previously reported RmSBP crystal at pH 4.5 belonged to monoclinic space group $C2_1$ [10].

Table 1. Data collection and refinement statistics.

Data collection	**pH 5.5**	**pH 6.0**	**pH 7.5**
Resolution	39.29-1.50 (1.53-1.50)	20.0—1.8 (1.87-1.8)	50.0-1.90 (1.93-1.90)
Space group	$P2_12_12_1$	$P2_122_1$	$P2_12_12_1$
Unique reflections	21337	12659	10511 (494)
Unit cell parameter			
a, b, c (Å)	46.42, 48.61, 58.11	34.91, 35.72, 115.57	46.54, 48.60, 57.82
Completeness (%)	99.2 (97.7)	90.5 (95.0)	95.5 (91.3)
Multiplicity	5.4 (4.9)	4.8 (4.9)	7.6 (4.2)
$I/\sigma(I)$	40.12 (5.57)	27.60 (6.20)	44.74 (4.09)
R_{merge}	0.065 (0.349)	0.118 (0.425)	0.101 (0.480)
R_{pim}	0.031 (0.170)	0.057 (0.198)	0.034 (0.245)
Refinement			
Resolution	37.29-1.50	14.94-1.80	37.20-1.90
R_{work}[a]	0.185	0.190	0.178
R_{free}[b]	0.218	0.220	0.228
Average B factor (Å^2)			
protein	22.15	22.95	35.58
R.m.s.deviations			
bonds	0.019	0.007	0.014
angles	1.983	1.203	1.680
Ramachandran			
preferred	98.66	98.7	98.7
allowed	1.34	1.30	1.3
PDB	6K1W	6K1X	6K1Y

Values in the parentheses refers to the highest resolution shell.

[a] $R_{work} = \Sigma||F_{obs}|-|F_{calc}||/\Sigma|F_{obs}|$, where F_{obs} and F_{calc} are the observed and calculated structure-factor amplitudes respectively.

[b] R_{free} was calculated as R_{work} using a randomly selected subset (10%) of unique reflections not used for structure refinement.

The structures of RmSBP at pH 5.5, 6.0, and 7.5 were refined up to 1.5 Å, 1.8 Å, 1.9 Å resolutions, respectively, and produced R_{work}/R_{free} of 18.5%/21.8%, 19.0%/22.0%, and 17.8%/22.8%, respectively. All RmSBP structures at pH 5.5, 6.0, and 7.5 were composed of six α-helices and six β-strands, and formed an α/β fold with extra domain at C-term (**Figure 2a**). Detailed structural topology information describing RmSBP had been previously reported [10]. Here, we described the novel finding for the peripheral flexible regions of RmSBP. Previously, we had classified RmSBP into one α/β domain [10]. However, in the present study, RmSBP was newly classified into α/β domain (α1-α4 and β1-β5) and C-term extended domain (α5, α6, β6 and β5) through comparative analysis with other homologous SBP structures (**Figure 1a and 2a**).

At all RmSBP structures at pH 5.5, 6.0, and 7.5, the electron density map of core of α/β domain of RmSBP was well defined, but peripheral loop and C-terminus were disordered or structurally flexible. In RmSBP-pH 5.5, electron density map for four amino acids (Asp151, Ala152, Glu153 and Gly154) at β4-β5 loop and five residues (Asp177 and Arg178) at α6-helix of C-terminal were disordered. In RmSBP-pH 6.0, electron density map for three residues (Asp151, Ala152, Glu153) at β4-β5 loop were disordered. In RmSBP-pH 7.5, although all residues were fitted into the electron density map without disordered electron density map, however structural flexibility with high

Preprints (www.preprints.org) | NOT PEER-REVIEWED | Posted: 27 September 2019 doi:10.20944/preprints201909.0313.v1

191 B-factor value was observed (see below). The superimposition of the crystal structures of RmSBP at
192 pH 5.5, pH 6.0 and pH 7.5 with previously reported crystal structure of RmSBP at pH 4.5 showed
193 similarity for whole Cα atoms (with r.m.s. deviation of 0.7196-1.3262), but two significantly different
194 conformations were observed. At β1- α2 loop, Cα atoms at pH 6.0 in the loop portion of the β1-α2
195 loop were shifted by about 2.0 Å compared to Cα atoms at other pH, and about 1.3 Å shifted to
196 α2-helix (**Figure 2b**). On the other hand, the extended C-term domain was not structurally aligned
197 (**Figure 2b**), and it was shifted by about 2.8 Å in α5-helix, and by 2.3 Å and 2.7 Å in loop and
198 C-terminal, respectively (**Figure 2b**).
199

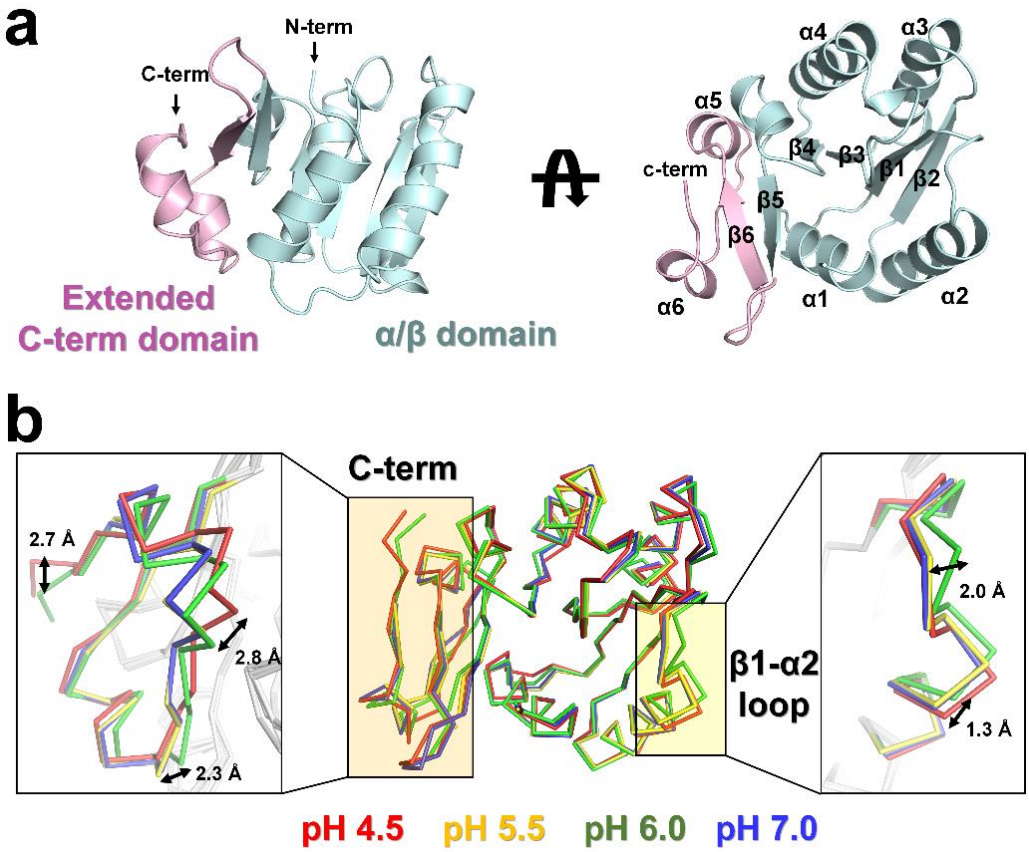

200

201 **Figure 2.** Crystal structure of RmSBPs. (a) Overall structure of RmSBP (pH 7.5) consists of α/β core
202 domain (cyan) and extended C-term domain (pink). (b) Superimposition of RmSBPs at pH 4.5 (red),
203 5.5 (yellow), 6.0 (green), and 7.5 (blue). Conformational differences of RmSBP are observed at β1-α2
204 loop (yellow transparency) and C-term domain (orange transparency).

205

206 Subsequently, we performed temperature B-factor analysis on all RmSBP structures (**Figure 3**). At
207 pH 4.5, RmSBP showed almost rigid fold except for the few N-terminus (**Figure 3a**). At pH 5.5, the
208 B-factor of RmSBP was relatively high at β1-α2 loop on α/β domain, and C-term domain was not
209 built due to lack of electron density map (**Figure 3a**). At pH 6.0, the overall α/β domain of RmSBP
210 showed a high rigidity, but it shows high B-factor value at the α6-helix in C-term domain (**Figure**
211 **3a**). At pH 7.5, there was no disordered electron density map of RmSBP similar to RmSBP structure
212 at pH 4.5, but relatively high flexibility was observed at β1-α2 loop and C-term domain (**Figure 3a**).
213 The analysis of normalized Cα atom B-factor for four RmSBP showed that β1-α2 loop, β5-β6 loop
214 and C-term helix had the relatively higher flexibility when compared with whole residues (**Figure**
215 **3b**). On the other hand, in the RmSBP structure, the portion of the electron density map with

Preprints (www.preprints.org) | NOT PEER-REVIEWED | Posted: 27 September 2019 doi:10.20944/preprints201909.0313.v1

disordered or relatively high b-factor area did not have a structural change in proportion of the acid or basic pH concentration.

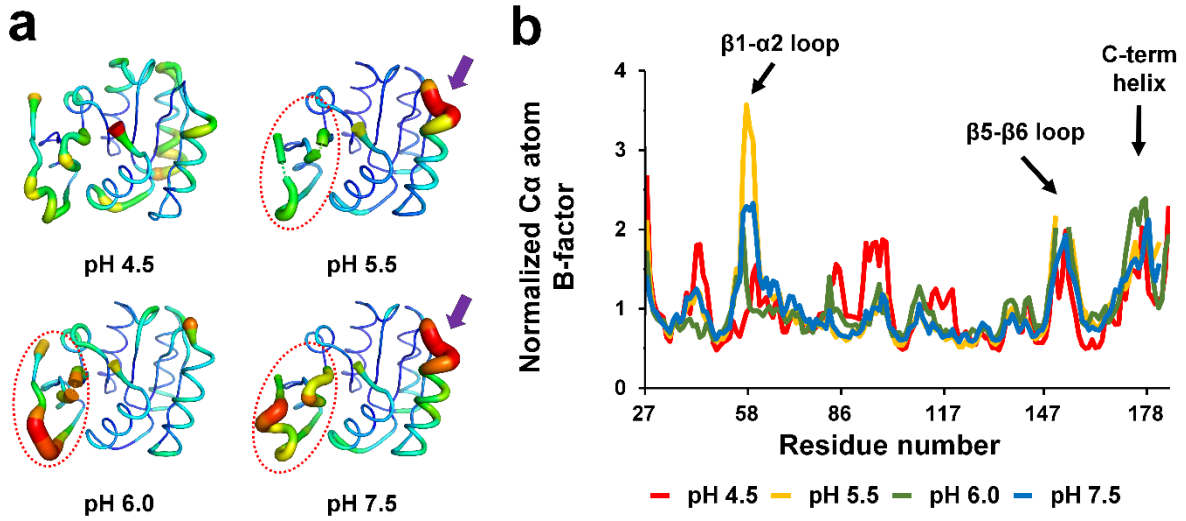

Figure 3. Analysis of flexible region of RmSBPs. (a) B-factor representation of RmSBP at pH 4.5, 5.5, 6.0, and 7.5. (b) Plot of normalized B-factor of Ca atoms of RmSBP at pH 4.5 (red), 5.5 (orange), 6.0 (green), and 7.5 (blue).

4. Discussion

We performed the comparative, computational and structural analysis of RmSBP for comprehensive understanding the molecular function of short length SBP. We previously described that the RmSBP consisted of single α/β domain, however, here we newly divided the RmSBP structure into α/β domain and extended C-term domain based on the comparative structural analysis. In particular, the C-term domain represented a unique topology in which RmSBP was distinguished from other SBP. In substrate binding model, four substrate binding sites were predicted, at positions important for the conformational changes required to recognize the substrate. However, since previously determined RmSBP at pH 4.5 exhibited a highly rigid structure showing a low level of B-factor value, there was no experimental evidence on whether the actual RmSBP was structurally flexible. To observe the structural flexibility of RmSBP, we crystallized and determined three crystal structures of RmSBP through three new crystallization conditions that had not been reported previously. The structural flexibility of β1-α2 loop, β5-β6 loop, and C-term helix of RmSBP may provide the initial framework for structural studies on short length SBP, as well as other SBP proteins. Although our study provides important information for understanding the structural properties of a short length SBP, further biochemical experiments on a variety of potential SBP substrates will need to be performed to understand their exact biological function. In this regard, not only finding substrates for RmSBP single proteins, but also in-depth study of their partner proteins and their functional relevance with the MCP around RmSBP proteins is required.

Author Contributions: J.E.B. performed cloning, and protein preparation. I.J.K. performed crystallization. Y.X analyzed the structures, and revised manuscript. K.H.N. performed data collection, structure determination, and wrote the manuscript.

Funding: This research was funded by the National Research Foundation of Korea (NRF-2017R1D1A1B03033087 and NRF-2017M3A9F6029736). This work was supported by Korea MSIT and PAL (Korea), and the Korea University Grant.

Acknowledgments: We thank the beamline staff at the MX beamlines at PLS-II at Pohang Accelerator Laboratory for assistance in data collection.

Conflicts of Interest: The authors declare no conflict of interest.

References

1. Maqbool, A.; Horler, R. S.; Muller, A.; Wilkinson, A. J.; Wilson, K. S.; Thomas, G. H., The substrate-binding protein in bacterial ABC transporters: dissecting roles in the evolution of substrate specificity. *Biochem Soc Trans* **2015,** 43, (5), 1011-7.
2. van der Heide, T.; Poolman, B., ABC transporters: one, two or four extracytoplasmic substrate-binding sites? *EMBO Rep* **2002,** 3, (10), 938-43.
3. Higgins, C. F., ABC transporters: from microorganisms to man. *Annu Rev Cell Biol* **1992,** 8, 67-113.
4. Berntsson, R. P.; Smits, S. H.; Schmitt, L.; Slotboom, D. J.; Poolman, B., A structural classification of substrate-binding proteins. *FEBS Lett* **2010,** 584, (12), 2606-17.
5. Tam, R.; Saier, M. H., Jr., Structural, functional, and evolutionary relationships among extracellular solute-binding receptors of bacteria. *Microbiol Rev* **1993,** 57, (2), 320-46.
6. Fukami-Kobayashi, K.; Tateno, Y.; Nishikawa, K., Domain dislocation: a change of core structure in periplasmic binding proteins in their evolutionary history. *J Mol Biol* **1999,** 286, (1), 279-90.
7. Scheepers, G. H.; Lycklama, A. N. J. A.; Poolman, B., An updated structural classification of substrate-binding proteins. *FEBS Lett* **2016,** 590, (23), 4393-4401.
8. Quiocho, F. A.; Ledvina, P. S., Atomic structure and specificity of bacterial periplasmic receptors for active transport and chemotaxis: variation of common themes. *Mol Microbiol* **1996,** 20, (1), 17-25.
9. Bjornsdottir, S. H.; Blondal, T.; Hreggvidsson, G. O.; Eggertsson, G.; Petursdottir, S.; Hjorleifsdottir, S.; Thorbjarnardottir, S. H.; Kristjansson, J. K., Rhodothermus marinus: physiology and molecular biology. *Extremophiles* **2006,** 10, (1), 1-16.
10. Bae, J. E.; Kim, I. J.; Kim, K. J.; Nam, K. H., Crystal structure of a substrate-binding protein from Rhodothermus marinus reveals a single alpha/beta-domain. *Biochem Biophys Res Commun* **2018,** 497, (1), 368-373.
11. Kelley, L. A.; Mezulis, S.; Yates, C. M.; Wass, M. N.; Sternberg, M. J., The Phyre2 web portal for protein modeling, prediction and analysis. *Nat Protoc* **2015,** 10, (6), 845-58.
12. Wass, M. N.; Kelley, L. A.; Sternberg, M. J., 3DLigandSite: predicting ligand-binding sites using similar structures. *Nucleic Acids Res* **2010,** 38, (Web Server issue), W469-73.
13. Park, S. Y.; Ha, S. C.; Kim, Y. G., The Protein Crystallography Beamlines at the Pohang Light Source II *Biodesign* **2017,** 5, (1), 30-34.
14. Otwinowski, Z.; Minor, W., Processing of X-ray diffraction data collected in oscillation mode. *Methods Enzymol* **1997,** 276, 307-26.
15. Adams, P. D.; Afonine, P. V.; Bunkoczi, G.; Chen, V. B.; Davis, I. W.; Echols, N.; Headd, J. J.; Hung, L. W.; Kapral, G. J.; Grosse-Kunstleve, R. W.; McCoy, A. J.; Moriarty, N. W.; Oeffner, R.; Read, R. J.; Richardson, D. C.; Richardson, J. S.; Terwilliger, T. C.; Zwart, P. H., PHENIX: a comprehensive Python-based system for macromolecular structure solution. *Acta Crystallogr D Biol Crystallogr* **2010,** 66, (Pt 2), 213-21.
16. Emsley, P.; Cowtan, K., Coot: model-building tools for molecular graphics. *Acta Crystallogr D Biol Crystallogr* **2004,** 60, (Pt 12 Pt 1), 2126-32.

17. Murshudov, G. N.; Skubak, P.; Lebedev, A. A.; Pannu, N. S.; Steiner, R. A.; Nicholls, R. A.; Winn, M. D.; Long, F.; Vagin, A. A., REFMAC5 for the refinement of macromolecular crystal structures. *Acta Crystallogr D Biol Crystallogr* **2011,** 67, (Pt 4), 355-67.
18. Afonine, P. V.; Grosse-Kunstleve, R. W.; Echols, N.; Headd, J. J.; Moriarty, N. W.; Mustyakimov, M.; Terwilliger, T. C.; Urzhumtsev, A.; Zwart, P. H.; Adams, P. D., Towards automated crystallographic structure refinement with phenix.refine. *Acta Crystallogr D Biol Crystallogr* **2012,** 68, (Pt 4), 352-67.
19. Chen, V. B.; Arendall, W. B., 3rd; Headd, J. J.; Keedy, D. A.; Immormino, R. M.; Kapral, G. J.; Murray, L. W.; Richardson, J. S.; Richardson, D. C., MolProbity: all-atom structure validation for macromolecular crystallography. *Acta Crystallogr D Biol Crystallogr* **2010,** 66, (Pt 1), 12-21.
20. The PyMOL Molecular Graphics System, Version 1.8 Schrödinger, LLC.